

# The genetic signature of rapid range expansions: How dispersal, growth and invasion speed impact heterozygosity and allele surfing



Devin W. Goodsman<sup>a,\*</sup>, Barry Cooke<sup>c</sup>, David W. Coltman<sup>a</sup>, Mark A. Lewis<sup>a,b</sup>

<sup>a</sup> Department of Biological Sciences, CW 405, Biological Sciences Bldg., University of Alberta, Edmonton, Alberta, Canada T6G 2E9

<sup>b</sup> Mathematical and Statistical Sciences, 632 CAB, University of Alberta, Edmonton, Alberta, Canada T6G 2G1

<sup>c</sup> Canadian Forest Service, Northern Forestry Centre, 5320 122 Street Northwest, Edmonton, Alberta, Canada T6H 3S5

## ARTICLE INFO

### Article history:

Received 6 December 2013

Available online 6 September 2014

### Keywords:

Dispersal  
Genetic diversity  
Heterozygosity  
Invasion  
Range expansion

## ABSTRACT

As researchers collect spatiotemporal population and genetic data in tandem, models that connect demography and dispersal to genetics are increasingly relevant. The dominant spatiotemporal model of invasion genetics is the stepping-stone model which represents a gradual range expansion in which individuals jump to uncolonized locations one step at a time. However, many range expansions occur quickly as individuals disperse far from currently colonized regions. For these types of expansion, stepping-stone models are inappropriate. To more accurately reflect wider dispersal in many organisms, we created kernel-based models of invasion genetics based on integrodifference equations. Classic theory relating to integrodifference equations suggests that the speed of range expansions is a function of population growth and dispersal. In our simulations, populations that expanded at the same speed but with spread rates driven by dispersal retained more heterozygosity along axes of expansion than range expansions with rates of spread that were driven primarily by population growth. To investigate surfing we introduced mutant alleles in wave fronts of simulated range expansions. In our models based on random mating, surfing alleles remained at relatively low frequencies and surfed less often compared to previous results based on stepping-stone simulations with asexual reproduction.

© 2014 Elsevier Inc. All rights reserved.

## 1. Introduction

Range expansions explain the wide spatial distribution of many dominant species. Unfortunately however, researchers often have only a snapshot of the extent of a recently expanded range rather than a complete spatiotemporal dataset. Genetic data have been used to elucidate processes underlying range expansions based on these snapshots, from our own planetary conquest (Ramachandran et al., 2005) to the post-glacial expansion of grasshoppers (Hewitt, 1999). Such insights, based on snapshots of genetic patterns on the landscape, are predicated on models that connect the dynamics, movement and genetics of populations. Thus, spatiotemporal genetic models are increasingly relevant as we accumulate large genetic databases. In this research we introduce integrodifference models as an alternative modeling framework in invasion genetics

with a sound mathematical and ecological basis. Integrodifference equations are discrete-time, continuous-space models that apply to range expansions in which populations have synchronized growth and dispersal stages (Neubert et al., 1995). Thus, they are useful for many herbaceous, invertebrate, and vertebrate species prone to invasion (Kot et al., 1996).

Currently, invasion models with analytical solutions for the patterns of genetic diversity that they produce are limited to the island model (Wright, 1951; Buerger and Akerman, 2011) and the stepping-stone model (Kimura and Weiss, 1964; Thibault et al., 2009; DeGiorgio et al., 2011; Slatkin and Excoffier, 2012). In the island model, subpopulations receive migrants at a constant rate from a single unchanging source population, whereas in the stepping-stone model, unoccupied demes are colonized sequentially one after another, and only receive migrants from adjacent subpopulations (Kimura and Weiss, 1964; DeGiorgio et al., 2009, 2011). Many dispersing organisms however, can move to locations beyond adjacent unoccupied areas (Levin et al., 2003) and dispersal is an important determinant of the speed of population expansion in space (Kot et al., 1996). For these reasons, neither the island nor the stepping-model in their original form is realistic in terms of population processes or dispersal (Le Corre and Kremer, 1998).

\* Corresponding author.

E-mail addresses: [goodsman@ualberta.ca](mailto:goodsman@ualberta.ca) (D.W. Goodsman), [Barry.Cooke@NRCan-RNCan.gc.ca](mailto:Barry.Cooke@NRCan-RNCan.gc.ca) (B. Cooke), [dcoltman@ualberta.ca](mailto:dcoltman@ualberta.ca) (D.W. Coltman), [mark.lewis@ualberta.ca](mailto:mark.lewis@ualberta.ca) (M.A. Lewis).

Realism has been added in modeling studies in a variety of ways. The stepping-stone model has been amended to include more realism by incorporating logistic population growth (Austerlitz et al., 1997). The consequences of Allee effects have also been explored in haploid model systems using the reaction–diffusion framework (Hallatschek and Nelson, 2008; Roques et al., 2012). The impact of stepping-stone, diffusive, and leptokurtic dispersal on genetic patterns has been explored by Nichols and Hewitt (1994) and by Ibrahim et al. (1996) using simulations featuring logistic population growth. Other simulation studies investigated differences between the effect of stratified and diffusive dispersal on the genetic structure of maternally inherited genes (Le Corre et al., 1997) and on genetic diversity along axes of range expansion (Bialozyt et al., 2006).

Results from simulations and simple models with analytical solutions underpin our understanding of how heterozygosity within populations decreases along axes of expansion (Austerlitz et al., 1997; Le Corre et al., 1997; Nichols and Hewitt, 1994). Heterozygosity reduction in expanding populations is a consequence of genetic drift that results from population bottlenecks at the front of range expansions (Austerlitz et al., 1997). Heterozygosity loss due to genetic drift can explain how genetic diversity is reduced at the front of expanding populations, but another mechanism called allele surfing (Edmonds et al., 2004; Hallatschek et al., 2007; Hallatschek and Nelson, 2010; Lehe et al., 2012) may explain why certain alleles persist there. In allele surfing, alleles and mutations that occur near the front of population expansions are able to proliferate and achieve higher frequencies than expected in populations at equilibrium (Excoffier and Ray, 2008). Most studies of allele surfing have focused on stepping-stone models with maternally inherited alleles, which is equivalent to asexual reproduction (Edmonds et al., 2004; Hallatschek et al., 2007; Hallatschek and Nelson, 2008; Lehe et al., 2012). Therefore, the importance of allele surfing in range expansions with other mating systems and wide dispersal has not been established.

In part due to wide dispersal, many biological invasions expand quickly rather than at the evolutionary time scales typically associated with human expansion out of Africa (Ramachandran et al., 2005) or with the expansion of oak trees in Europe (Hewitt, 1999). Therefore ecologists are often interested in understanding processes that underly expansions that have occurred over ecological time scales of tens of years rather than over thousands of years. The speed at which populations expand in space is determined by demographic growth and dispersal (Kot et al., 1996) and therefore models that clearly connect invasion speeds to these population traits are essential when studying rapid range expansions. Using integrodifference equations as the basis for our investigation of the genetic signature of range expansions allowed us to compute theoretical invasion speeds from demographic growth and dispersal parameters using classic theory (Kot et al., 1996).

The primary objective of this research was to study genetic diversity patterns arising in rapid range expansions. We therefore used integrodifference equation-based models to simulate over relatively short time periods with wide dispersal kernels that overlapped many demes. We compared the relative impacts of demographic growth and dispersal on the genetic signatures of range expansions spreading at the same speed, explored the genetic consequences of varying diffusivity in expansions with identical demography, simulated anisotropic range expansions in two spatial dimensions, and compared heterozygosity patterns as well as the distribution of surfing alleles produced by simulated range expansions with a variety of dispersal kernels. As much of the previous work on allele surfing in range expansions has focused on asexual or haploid model systems, we also contrasted results from simulations with random mating to those with asexual mating.

## 2. Models

### 2.1. Population dynamics and spread models

We consider a species with Beverton–Holt population dynamics (Beverton, 1957). The species reproduces synchronously before dispersing in space according to a dispersal kernel  $k(x - y)$ , which describes the probability that an animal moves from location  $y$  to location  $x$ . The resulting integrodifference model is

$$f(N_t(y)) = \frac{R_0(N_t(y))}{1 + (R_0 - 1)N_t(y)/K}, \quad y \in \Omega, \quad (1a)$$

$$N_{t+1}(x) = \int_{\Omega} k(x - y)f(N_t(y))dy, \quad (1b)$$

where  $N_t(x)$  is the population density in space at time  $t$ ,  $R_0$  is the geometric growth parameter and  $K$  is the carrying capacity. The infinite one-dimensional spatial domain is represented by  $\Omega$ .

The dispersal kernel formulation is very flexible and a variety of dispersal behaviors can be modeled by changing it (Neubert et al., 1995). The assumption of spatially homogenous diffusive dispersal is embodied in the Gaussian dispersal kernel:

$$k(x - y) = \frac{1}{\sqrt{4\pi D}} \exp\left(\frac{-(x - y)^2}{4D}\right), \quad (2)$$

where  $D$  is the diffusion constant. Note our diffusion constant represents  $Dt$  in standard formulations of random-walk-based diffusion models (Codling et al., 2008). This diffusion constant can be derived based on the probability that an individual will jump to the right, to the left, or not move (Codling et al., 2008). Although it is tempting to use diffusion to describe all animal movement, dispersal in many species is better approximated using leptokurtic distributions (Walters et al., 2006; Skarpaas and Shea, 2007) in which individuals have a higher probability of dispersing short and long distances than in a Gaussian kernel with the same variance. Therefore, we also simulate range expansions with double exponential (Laplace) and fat-tailed kernels, both of which are leptokurtic.

The Laplace kernel, when derived based on a diffusive model with constant settling (Neubert et al., 1995), has the form

$$k(x - y) = \frac{1}{2} \sqrt{a/D} \exp(-\sqrt{a/D}|x - y|), \quad (3)$$

where  $D$  is the diffusion constant as before,  $a$  is the constant settling rate, and  $k(x - y)$  describes the distribution of settled individuals.

Fat-tailed dispersal kernels are those without exponentially bounded tails. Authors have argued based on simulation studies that longer-distance dispersal is increasingly selected for over the course of invasions leading to the evolution of fat-tailed kernels (Phillips et al., 2008). A typical fat-tailed kernel comes from Wallace (1966) and Taylor (1978) who described the relationship between distance from a release point and density of fruit flies using

$$k(x - y) = \frac{\alpha^2}{4} \exp(-\alpha\sqrt{|x - y|}), \quad (4)$$

where  $\alpha$  determines the rate of decrease with the square root of distance.

For kernels with moment-generating functions such as (2) and (3), the model equation (1) has traveling wave solutions that connect the zero equilibrium in front of the wave to the carrying capacity equilibrium at the top of the wave (Kot et al., 1996). For range expansions that have these traveling wave solutions, we can compute the minimum traveling wave speed. Locally introduced populations that grow and spread according to the Gaussian kernel (2) have a minimum traveling wave speed  $c(R_0, D) = 2\sqrt{D \ln(R_0)}$

(Kot et al., 1996). The expression for spreading speed for models with the Laplacian kernel (3) is more complicated and must be solved numerically by minimizing  $\{(1/s)\ln(R_0/(1 - s^2D/a))\}$  on the interval  $s \in (0, \sqrt{a/D})$  (Kot et al., 1996). In this study, we sometimes standardize the traveling wave speed of simulations to investigate the relative impacts of dispersal and population growth on the spatial genetics of range expansions traveling at the same speed.

Unlike integrodifference equations with kernels that have moment generating functions, integrodifference equation models with fat-tailed kernels (4) give rise to continually accelerating invasions with asymptotically infinite spreading speeds (Kot et al., 1996). This means that spreading speeds increase over time—a phenomenon that may seem counter-intuitive, but which has been observed in natural invasions and attributed to the evolution of more frequent long-distance dispersal over the course of the invasion (Phillips et al., 2008).

To illustrate the effect of anisotropic dispersal on heterozygosity, we construct a two-dimensional model similar to (1):

$$f(N_t(\mathbf{y})) = \frac{R_0(N_t(\mathbf{y}))}{1 + (R_0 - 1)N_t(\mathbf{y})/K}, \quad \mathbf{y} \in \mathbf{R}^2, \quad (5a)$$

$$N_{t+1}(\mathbf{x}) = \int_{\mathbf{R}^2} k(\mathbf{x} - \mathbf{y})f(N_t(\mathbf{y}))d\mathbf{y}. \quad (5b)$$

Here  $\mathbf{y}$  is the vector  $(y_1, y_2)$  and  $k(\mathbf{x} - \mathbf{y})$  is the kernel describing the probability of moving from  $\mathbf{y}$  to location  $\mathbf{x} = (x_1, x_2)$ :

$$k(\mathbf{x} - \mathbf{y}) = (C) \exp\left(\frac{-[(x_1 - y_1)^2 + b(x_2 - y_2)^2]}{4D}\right), \quad (6)$$

which is the two-dimensional analog of (2) except that diffusivity in the  $x_1$  direction is  $b$  times that in the  $x_2$  direction and  $C$  is the normalization constant that ensures that the density sums to one. If  $b \neq 1$ , in (6) the integrodifference equation model (5) produces populations expanding at different speeds in different directions.

## 2.2. Stochastic discretized model

To simulate (1) on a computer, it is necessary to discretize in space, leading to a coupled map lattice:

$$f(N_t(y)) = \frac{R_0(N_t(y))}{1 + (R_0 - 1)N_t(y)/K}, \quad y \in \mathbb{Z}, \quad (7a)$$

$$N_{t+1}(x) = \sum_{y=1}^u k(x - y)f(N_t(y)), \quad (7b)$$

where the spatial domain is now divided into  $u$  equal segments. The two-dimensional analog of (1) can be discretized in two-dimensional space in an analogous way.

The birth component of (7a) given by  $f(N_t(y))$  is a model for the density of individuals within a given segment of the discretized domain. To accommodate the stochastic genetics model we need an integer number of individuals in each segment. Therefore, we assume that birth is a stochastic Poisson process within each segment with mean  $\lambda_t(y) = f(N_t(y))$ . Thus, the number of individuals in the next generation is a Poisson distributed random variable  $X_{t+1/2}(y)$  resulting in a stochastic coupled map lattice

$$X_{t+1/2}(y) \sim \text{Poisson}(\lambda_t(y) = f(N_t(y))), \quad (8a)$$

$$N_{t+1}(x) = \sum_{y=1}^u k(x - y)X_{t+1/2}(y). \quad (8b)$$

## 2.3. Genetics model

We overlaid a genetics model based on a hermaphroditic diploid species in which we considered a single neutral biallelic locus on top of the stochastic coupled map lattice. This is a standard genetics model used for investigating the dynamics of neutral alleles that avoids the more complicated mating dynamics in two-sex systems. The current version of the model does not include random mutation. Instead, to investigate the fate of mutations that initially occur in the wave front, we introduced mutations at specific locations at the front of population expansions, and then followed their distribution over multiple stochastic simulations of our model (see Section 3.4: Simulating surfing).

The species mates according to the laws of random mating meaning that any allele at a particular location is equally likely to pair with any other allele at the same location (Gillespie, 2004). Thus, to determine the genotype of each new individual we drew from a multinomial distribution:

$$N_{t+1/2}^{AA,AB,BB}(y) \sim \text{Multinom}(X_{t+1/2}(y), \mathbf{p}) \quad (9)$$

where  $N_{t+1/2}^{AA,AB,BB}(y)$  is the number of individuals in each genotype (AA, AB, or BB) at location  $y$ ,  $X_{t+1/2}(y)$  is the Poisson random variable used in (8), and  $\mathbf{p}$  is a vector of probabilities  $\mathbf{p} = ([\rho_t(y)]^2, 2[\rho_t(y)][1 - \rho_t(y)], [1 - \rho_t(y)]^2)$ . The frequency of the A allele at time  $t$  and location  $y$  is  $\rho_t(y)$ . Now, rather than redistributing individuals as in (8), the coupled map lattice redistributes individuals of each genotype as follows:

$$N_{t+1}(x) = \sum_{y=1}^u k(x - y)N_{t+1/2}^{AA,AB,BB}(y). \quad (10)$$

After individuals have been redistributed, a new  $\rho_{t+1}(x)$  is calculated:

$$\rho_{t+1}(x) = \frac{N_{t+1}^{AA}(x) + 0.5N_{t+1}^{AB}(x)}{N_{t+1}^{AA}(x) + N_{t+1}^{AB}(x) + N_{t+1}^{BB}(x)}, \quad (11)$$

where  $N_{t+1}^{AA}(x)$  is the number of individuals with the AA genotype at time  $t + 1$  and location  $x$ . At the next iteration  $\rho_{t+1}(x) \rightarrow \rho_t(y)$ , which is a parameter in (9).

## 3. Methods

### 3.1. Simulation algorithm

We simulated the coupled map lattice with overlaid genetics using a spatial domain running in increments of  $800/2^{14}$  from  $-400$  to  $400$ . Fast Fourier transforms facilitated the computation of the convolution in (10). The boundaries were reflecting but the size of the domain was chosen such that the spreading population was far from the domain limits over the entire simulation period. We ran 100 Monte Carlo simulations of each invasion model to generate mean population and heterozygote densities at each location in our spatial domain at each generation. Example R (R Core Team, 2013) code for this simulation parallelized using the parallel package in R is provided in the online supplement (see Appendix B).

#### 1. set-up

- We started with a density of  $K$  (carrying capacity) individuals distributed around the center of the spatial domain and defined an initial allele frequency for these sub-populations ( $\rho_0(x_i)$ ).
- We fast Fourier transformed (FFT) the dispersal kernel using the FFT function in the base installation of R (Singleton, 1969). Note this only needed to be done once and the same FFT transformed dispersal kernel was used in each iterative step described below.

2. At each time iteration we simulated local population dynamics using (7a), then drew from a Poisson distribution as in (8a) to compute the number of new individuals at each location ( $X_{t+1}(y)$ ).
3. We then drew from a multinomial distribution with number of trials equal to  $X_{t+1}(y)$  and probability of drawing the A allele given by  $\rho_t(y)$  as in (9).
4. We redistributed individuals of each genotype by convolving their distribution on the landscape with the dispersal kernel. To do this we used the convolution theorem and multiplied the FFT for the dispersal kernel by the FFT of the distribution of each genotype before inverse fast Fourier transforming the result and shifting the convolution to center it.
5. We then computed the new frequency of the A allele at each location using (11). This allele frequency was then used to initialize the next iteration of random mating (return to step 2).

In all of our one-dimensional simulations we initialized the simulations by placing  $K = 40$  individuals in the 3 central locations in the one-dimensional domain each with a starting frequency of the A allele of  $\rho = 0.5$ .

### 3.2. Two-dimensional simulations

Our simulation algorithm for our two-dimensional model was similar to the algorithm for our one-dimensional model except that due to increased computational burden, we simulated on a domain running in increments of  $50/2^{10}$  from  $-25$  to  $25$  in both the  $x$  and  $y$  directions. We chose this domain size such that the area of our grids, or equivalently the size of our demes, would be equal to the square of the length of our demes in the one-dimensional simulations. Thus heterozygosity patterns generated in our one dimensional simulations could be compared to marginals generated by our two-dimensional simulations in either the  $x$  or  $y$  direction.

The simulation algorithm for two-dimensional range expansions is identical to the one-dimensional simulation algorithm except we initialized our two-dimensional simulation by placing  $K = 40$  individuals in the 9 central grid squares in our square domain, each with a frequency of the A allele of  $\rho = 0.5$ .

### 3.3. Comparing range expansion models

To compare the effect of population growth to the effect of dispersal on heterozygosity within sub-populations, we standardized so that invasions were progressing at the same speed, but one simulation featured faster growth and the other, higher dispersal. However, to compare the genetic signature of Gaussian, Laplace and fat-tailed dispersal kernels, we were unable to standardize in this way because the fat-tailed kernel leads to asymptotically infinite spreading speeds (Kot et al., 1996). Therefore, we standardized the kernels by matching their second central moments (equivalent to variance). The second central moments of the Gaussian, Laplace and fat-tailed kernels respectively are  $2D$ ,  $2D/a$ , and  $5!/a^4$  where the parameters are the same as defined in (2, 3, and 4).

We initially simulated range expansions for 50 generations with kernels with standardized second central moments. Due to different spreading speeds, the maximum extent of each simulated expansion varied. Most population genetics data, however, consist of snapshots of genetic patterns over a given spatial area. For this reason it may sometimes be more relevant to compare patterns generated over the same spatial extent. We therefore also standardized the extent of simulated range expansions generated by the different kernels by running the simulations for different numbers of generations.

To compute the number of generations needed for the simulated populations to expand over similar spatial extents, we compared the distance covered by simulated range expansion featuring

each of the dispersal kernels after 50 generations. After 50 generations the numerical solutions for simulations featuring each kernel were traveling wave solutions. Therefore the inflection point of each wave profile (where the wave profile was equal to half the carrying capacity), could be used to determine relative expansion in the different simulations. Using these inflection points, we computed the difference between the distance traveled after 50 generations by simulations with the fat-tailed kernel and Gaussian and Laplace kernels. Then, knowing the theoretical spreading speeds of range expansions featuring Gaussian and Laplace kernels, we were able to compute how many additional generations were required for these slower range expansions to cover the same extent as the fat-tailed simulation. A table detailing the various standardizations used in the figures is provided in the [Appendix](#).

### 3.4. Simulating surfing

To simulate surfing we initialized populations as described in our simulation algorithm above with one difference. Instead of initializing with  $\rho = 0.5$ , we initialized with only B alleles ( $\rho = 0$ ) such that all individuals were homozygous for the B allele. We simulated range expansions with Gaussian and Laplace kernels until generation 11. By generation 11 all of our simulations had reached constant spreading speeds and had traveling wave solutions. We then introduced a single A allele at a location in the traveling wave where the population density was one individual per unit length of our spatial domain at the very front of our traveling wave. We were able to track the location of the descendants of this introduced allele over time. We simulated for only 20 generations and we were therefore able to use a smaller spatial domain running from  $-100$  to  $100$  divided into increments of  $200/2^{12}$ . All other details were identical to those described above.

For comparison, we also simulated surfing for an asexually reproducing haploid organism by modifying our simulation algorithm as follows. Instead of drawing from a multinomial distribution, we drew from a binomial distribution to determine the number of individuals in the next generation that possessed the A allele:  $N_{t+1/2}^A(y) = \text{Binom}(X_{t+1/2}(y), \mu_t(y))$ , where  $\mu_t(y)$  is the frequency of the A allele at location  $y$  given by  $\mu_t(y) = N_{t+1}^A(y) / (N_{t+1}^A(y) + N_{t+1}^B(y))$ . We then redistributed individuals possessing either the A or B allele using a convolution as before and computed the new frequency of the A allele at each location to proceed to the next iteration of the model.

## 4. Calculations

When simulating over only a few generations, as we have done for surfing, it is worthwhile to compare deterministic solutions for the prevalence of the surfing allele to stochastic simulations. To compute deterministic solutions, we ignore genetic drift to arrive at the following system of integrodifference equations for a range expansion with individuals mating at random:

$$f(N_t(y)) = \frac{R_0(N_t(y))}{1 + (R_0 - 1)N_t(y)/K}, \quad y \in \Omega, \quad (12a)$$

$$AA_{t+1}(x) = \int_{\Omega} k(x-y)(\rho_t(y))^2 f(N_t(y)) dy, \quad (12b)$$

$$AB_{t+1}(x) = \int_{\Omega} k(x-y)2\rho_t(y)(1-\rho_t(y))f(N_t(y)) dy, \quad (12c)$$

$$BB_{t+1}(x) = \int_{\Omega} k(x-y)(1-\rho_t(y))^2 f(N_t(y)) dy, \quad (12d)$$

$$N_{t+1}(x) = AA_{t+1}(x) + AB_{t+1}(x) + BB_{t+1}(x), \quad (12e)$$

$$\rho_{t+1}(x) = \frac{2AA_{t+1}(x) + AB_{t+1}(x)}{2N_{t+1}(x)}, \quad (12f)$$

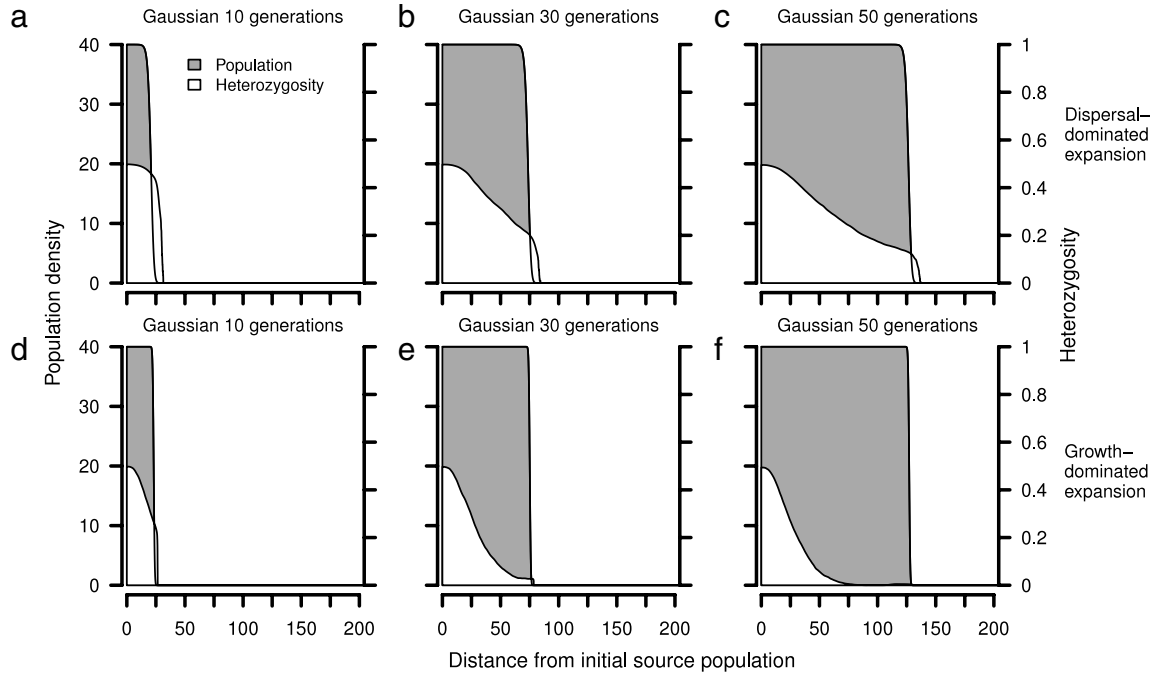


**Fig. 1.** Dispersal-dominated range expansions exhibit less loss of heterozygosity along the axis of expansion than growth-dominated range expansions. Numerical solutions of Eqs. (2) and (8)–(11) are shown with the dispersal-dominated range expansion (a)–(c) simulated with  $R_0 = 10$ ,  $K = 40$ , and  $D = 0.8$ , while the growth-dominated range expansion (d)–(f) was simulated with  $R_0 = 10,000$ ,  $K = 40$ , and  $D = 0.2$ . Both range expansions have theoretical invasion speeds of 2.71 units/generation and were initialized with 40 individuals at the origin and 40 individuals on either side of the origin all with a frequency of the A allele of 0.5.

where  $AA_{t+1}(x)$ ,  $AB_{t+1}(x)$  and  $BB_{t+1}(x)$  are the density of AA, AB and BB genotypes at location  $x$  and time  $t + 1$ . Deterministic solutions of this system can be compared to stochastic simulations to determine the impact of stochasticity on the location and abundance of rare alleles introduced at the wave front.

Similarly for an asexual haploid population we can write the following system of equations

$$f(N_t(y)) = \frac{R_0(N_t(y))}{1 + (R_0 - 1)N_t(y)/K}, \quad y \in \Omega, \quad (13a)$$

$$A_{t+1}(x) = \int_{\Omega} k(x - y)\mu_t(y)f(N_t(y))dy, \quad (13b)$$

$$B_{t+1}(x) = \int_{\Omega} k(x - y)(1 - \mu_t(y))f(N_t(y))dy, \quad (13c)$$

$$N_{t+1}(x) = A_{t+1}(x) + B_{t+1}(x), \quad (13d)$$

$$\mu_{t+1}(x) = A_{t+1}(x)/(N_{t+1}(x)). \quad (13e)$$

## 5. Results

### 5.1. Gradients in expected heterozygosity

During and after invasions simulated using our kernel-based models, heterozygosity always decreased along the axis of expansion in the direction of spread. In invasions traveling at the same speed, heterozygosity declined more gradually in expansions driven by population growth than in expansions driven by dispersal (Fig. 1). Eventually, because no mutation restored genetic diversity in the population, the heterozygotes went extinct near the expansion front (Fig. 1(f)). As a result, mean heterozygosity at the front of the expansion monotonically approached zero, and in the long term, the spatial pattern of heterozygosity resembled a normal distribution (Fig. 1(f)).

The leptokurtic double exponential kernel led to faster range expansions (Fig. 2(b)) and more heterozygosity retained along the

axis of spread (Fig. 2(b) and (e)) than did diffusive kernels with the same second moment (Fig. 2(a) and (d)). This effect was even stronger for the leptokurtic fat-tailed kernel (Fig. 2(c) and (f)).

In expansions with the same growth parameters but different dispersal parameters the slower invaders dispersed less extensively and therefore, lost heterozygosity relatively quickly along the axis of expansion compared to an invasion in which organisms were more dispersive (Fig. 3). Similarly, in our anisotropic dispersal simulations in two spatial dimensions, steeper declines in heterozygosity occurred in directions that corresponded to slower expansion rates (Fig. 4). Heterozygosity gradients along transects in our two-dimensional simulations were, however, much less pronounced than in comparable one-dimensional simulations (Fig. 4 versus Fig. 3).

Regions that were visually separable due to differences in allele frequency were evident when plots of the frequency of the A allele were plotted after a single stochastic realization of a range expansion (Fig. 5). However, these patterns were smoothed over when we averaged over 100 Monte Carlo simulations and computed heterozygosity as we have done in the majority of our graphics.

### 5.2. Mutant alleles

Dispersal-dominated range expansions retained more mutant alleles than growth-dominated range expansions traveling at the same speed (Fig. 5) after they were introduced in wave fronts. In dispersal-dominated expansions, introduced mutant alleles followed along with advancing waves for a few generations as can be seen in Fig. 5(a)–(c) in the right-skewed distribution of mutant alleles. Thus, mutants that initially occurred in waves driven by dispersal kernels with larger diffusion constants are able to persist in the wave longer (Fig. 5(a)–(c)) than mutants that initially occurred in waves driven by population growth (Fig. 5(e)–(f)). Note that even in the simulation experiment in which the mutant allele persisted much longer (Fig. 5(a)–(c)), its maximum frequency at any location was much less than the frequency at which it was originally introduced in the population ( $\rho = 1/2$ ).

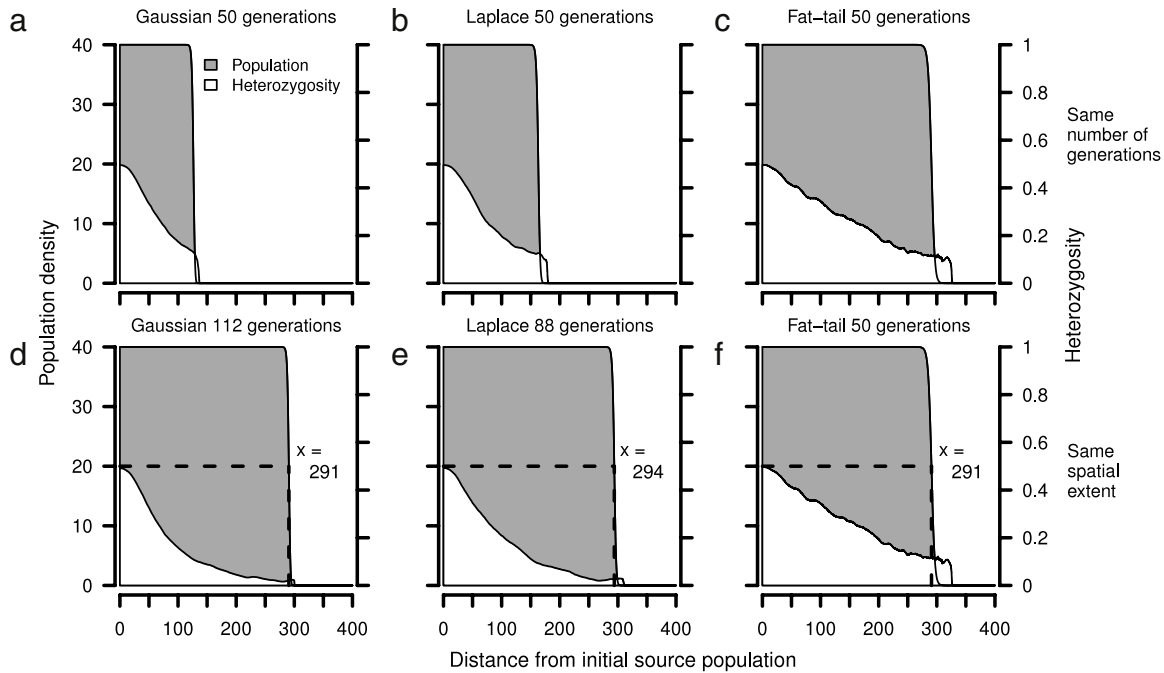


**Fig. 2.** Range expansions with leptokurtic and fat-tailed dispersal kernels exhibit less loss of heterozygosity along the axis of expansion than range expansions with Gaussian kernels with the same variance. Numerical solutions of Eqs. (8)–(11) with the Gaussian kernel (2) with  $D = 0.8$ , the Laplace kernel (3) with  $D = 0.8$  and  $a = 1$ , and the fat-tailed kernel (4) with  $\alpha = 2.94$ . Simulations with each kernel were run for 50 generations (a)–(c) or until the inflection point of the traveling population wave corresponded to  $x \approx 291$  (d)–(f). All range expansions were simulated with  $R_0 = 10$ ,  $K = 40$  and were initialized with 40 individuals at the origin and 40 individuals on either side of the origin all with a frequency of the A allele of 0.5.

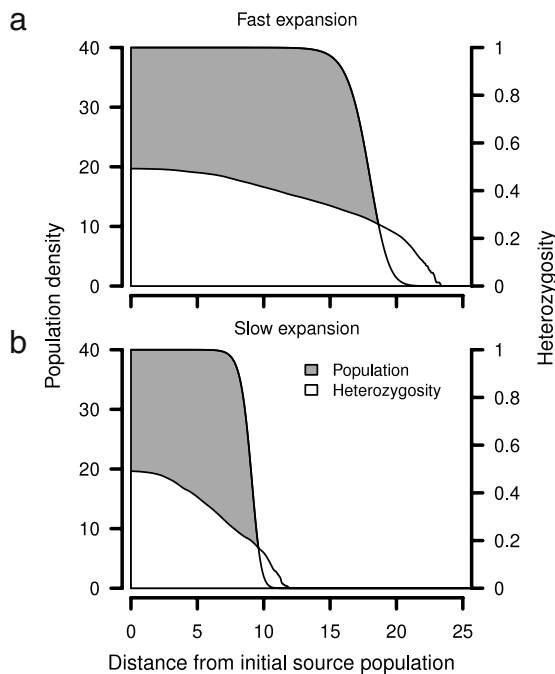


**Fig. 3.** Range expansions with Gaussian kernels with lower diffusivity exhibit more rapid loss of heterozygosity along the axis of expansion than range expansions with Gaussian kernels with higher diffusivity. Numerical solutions of Eqs. (2) and (8)–(11) with (a)  $R_0 = 2$ ,  $K = 40$ ,  $D = 0.1$ , (b)  $R_0 = 2$ ,  $K = 40$ ,  $D = 0.025$  and (c) their heterozygosities. Fast and slow invasions had theoretical invasion speeds of 0.53 and 0.26 units/generation respectively. Both simulations were initialized with 40 individuals at the origin and 40 individuals on either side of the origin all with a frequency of the A allele of 0.5. The fast and slow expansion simulations were both run for 40 generations.

In 1000 Monte Carlo simulations of the range expansion shown in Fig. 6(c), surfers maintained populations higher than 5% in the

wave front in only 3 simulations (Fig. 7). Even in simulations in which the surfing allele kept up with the wave front and maintained a frequency higher than 5%, the maximum frequency of the mutant allele was approximately 0.1 (Fig. 7).

Rare alleles occurring at the front of traveling waves of asexually reproducing organisms increase more than in organisms reproducing by random mating (Fig. 8(a)) even when the mutant initially occurs further behind the front of the wave such that the initial frequency of the mutant is 0.5 as in the diploid surfing simulations (Fig. 8(b)).

In both the random mating and the asexual surfing simulations, the mean spatial distribution of mutant alleles at any time was very well described by deterministic solutions of equations ((12) and (13) respectively) (Fig. 8(a) and (b)). Thus, cases in which the mutant allele surfed to frequencies above those predicted by the deterministic integrodifference equation were balanced by cases in which the mutant allele decreased to frequencies below those predicted by the deterministic model leading to the concordance between the predictions of the deterministic model and the expected density of mutant alleles at any location.

## 6. Discussion

Population growth and dispersal are important determinants of the speed of traveling waves in integrodifference models of range expansions. In our simulations, fast range expansions resulted in higher heterozygosity retention along the axis of spread than slow range expansions. The amount of heterozygosity retained depended not only on the speed of expansion, but also on whether the spread rate was primarily dispersal driven or growth driven. Population growth and dispersal were also important determinants of the eventual abundance of mutant alleles that originated in the wave front. Dispersal-dominated range expansions traveling at the same speed as growth-dominated range expansions had higher mean abundances of mutant alleles at any time after they were introduced. Mean abundances of mutant alleles must

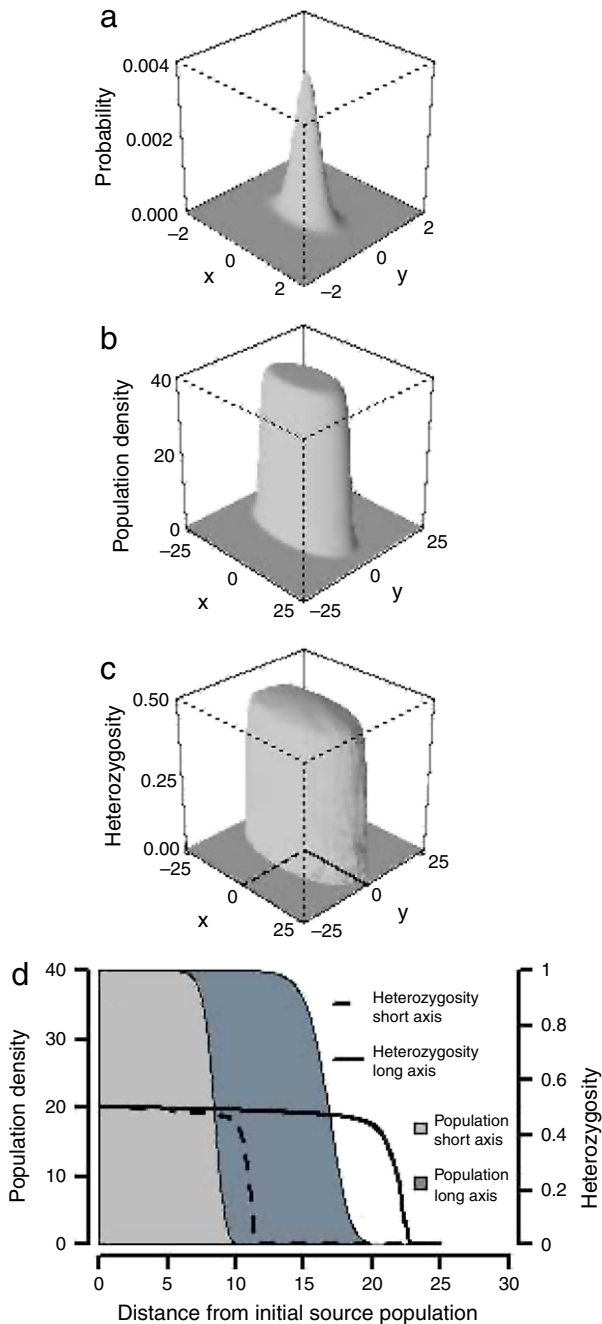


**Fig. 4.** An (a) anisotropic dispersal kernel (Eq. (6) with  $D = 0.1$ , and  $b = 4$ ) combined with Beverton–Holt population dynamics with  $R_0 = 2$  and  $K = 40$  leads to (b) an anisotropic range expansion with (c)–(d) steeper declines in heterozygosity in directions of slow expansion than in directions of fast expansion. Lines at the base of (c) represent transects in directions of fastest and slowest expansion. The surface plots (b) and (c) show numerical solutions of a spatially discretized version of (5) with stochastic population growth as in (8) and genetics as in Eqs. (9)–(11). The model was simulated for 40 generations after it was initialized with 40 individuals in each of the nine central grid squares around the origin and with a frequency of the A allele of 0.5.

be distinguished from rare surfing alleles that are able to remain in the population wave. For these surfing alleles, we found that in expanding populations with genetic recombination and kernel-based redistribution of individuals, the frequency of surfing alleles in the wave front was much lower than surfing results reported for stepping-stone models with asexual reproduction.

The shape of the dispersal kernel underlying population range expansions changes both the invasion speed and the rate of het-

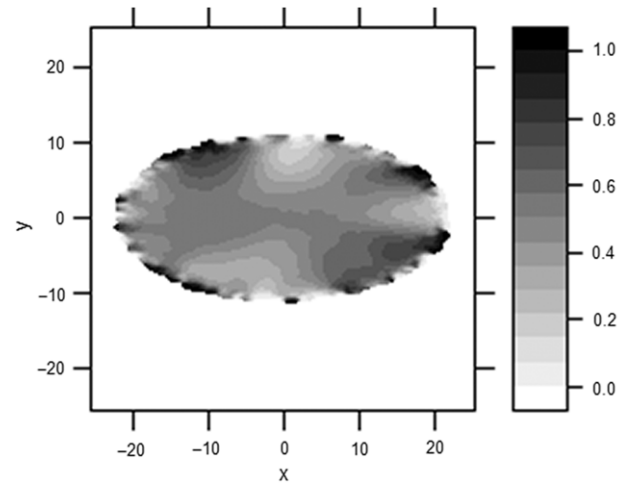


**Fig. 5.** After a single realization of the anisotropic two-dimensional range expansion with parameter values as in Fig. 4, sectors of genetically similar regions in the colonized spatial domain were evident only if a single simulation is depicted (without averaging over multiple simulations).

erozygosity loss along the axis of range expansion. Gaussian redistribution kernels with larger diffusion terms (larger variance) resulted in slower heterozygosity loss as the range expansion progressed than narrower Gaussian kernels even when invasions were traveling the same speed. Because leptokurtic dispersal kernels permit demes further behind the expansion front to contribute more genetic material to demes located at the wave front, range expansions with the same growth parameters and leptokurtic kernels resulted in higher heterozygosity retention than diffusive kernels with the same variance. As demes behind the wave-front are generally more heterozygous, leptokurtic kernels enable better mixing in pushed population waves, thereby reducing heterozygosity decay. Dispersal in many plants and insects is leptokurtic with dispersal characteristics resembling those in our simulations (Kot et al., 1996; Walters et al., 2006; Skarpaas and Shea, 2007). Consequently, when species with leptokurtic dispersal expand their ranges, we expect to see little loss of heterozygosity—especially when range expansions are sudden.

Range expansion with leptokurtic kernels produced gradually decreasing heterozygosity suggesting a smooth pattern in the distribution of genotypes on the landscape. This finding contrasts the findings of Ibrahim et al. (1996) whose simulation results suggested that leptokurtic kernels led to pockets of similar genotypes on the landscape. Differences between our findings and those of Ibrahim et al. (1996) are likely due to our use of Monte Carlo techniques to remove variability from overall trends. Examining a few outcomes of stochastic simulations as Ibrahim et al. (1996) have done reveals trends that are the result of stochastic interactions whereas Monte Carlo approaches smooth over the stochasticity and reveal the deterministic drivers of overall patterns. In addition, stochasticity is slightly different in our models than in those of Ibrahim et al. (1996). In their models, whether or not individuals leave their current demes is also random, and individuals had a relatively low probability of dispersing (0.05), whereas in our models all individuals dispersed according to the deterministic dispersal kernel. Consequently, our models are likely more representative of broad trends in highly dispersive species while the models of Ibrahim et al. (1996) are likely more representative of fine scale patterns generated by less vagile species.

Many organisms disperse asymmetrically in space (Gammon and Maurer, 2002; Munoz et al., 2004; Austerlitz et al., 2007; Morin et al., 2009) and therefore, their populations expand faster in some directions than in others. This occurs naturally when organisms are dispersing outwards from a port of entry or within

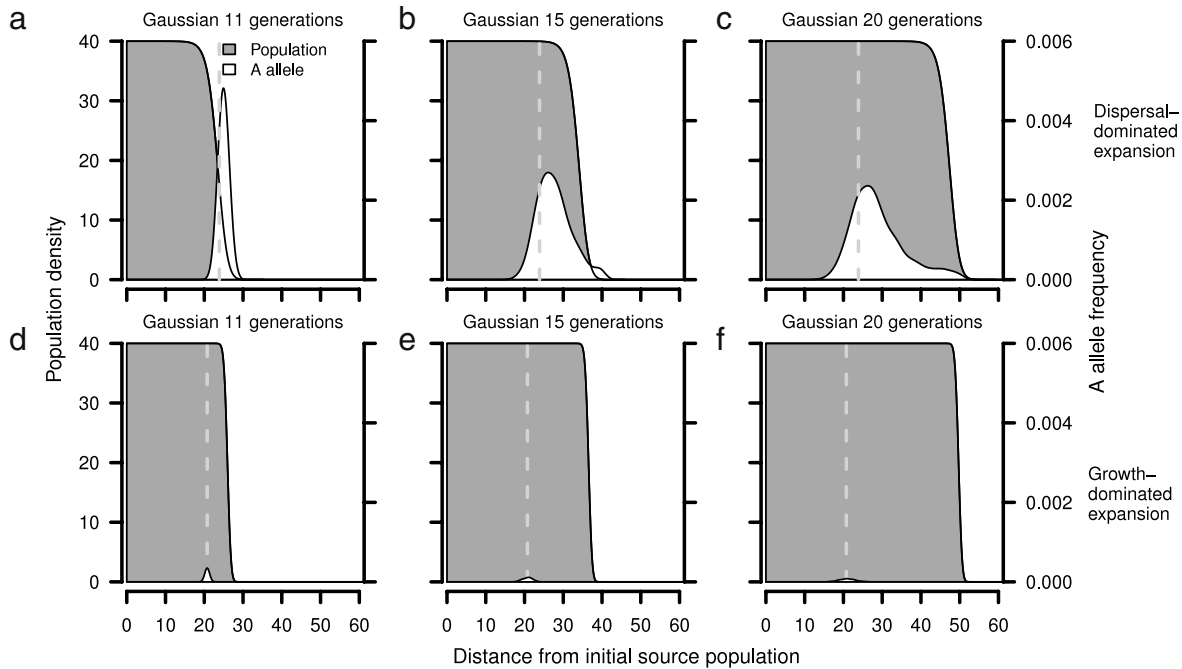


**Fig. 6.** Rare alleles or mutations that occur at the front of the traveling wave persist longer and in larger numbers in dispersal-dominated expansions than in growth-dominated expansions. Numerical solutions of Eqs. (2) and (8)–(11) are shown with the dispersal-dominated range expansion (a)–(c) simulated with  $R_0 = 10$ ,  $K = 40$ , and  $D = 0.8$ , while the growth-dominated range expansion (d)–(f) was simulated with  $R_0 = 10,000$ ,  $K = 40$ , and  $D = 0.2$ . Both range expansions have theoretical invasion speeds of 2.71 units/generation and were initialized with 40 individuals at the origin and 40 individuals on either side of the origin all with a frequency of the A allele of 0 (All individuals possessed only the B allele). In generation 11, a single A allele was introduced at the location in the traveling wave where the population density was approximately one individual per unit length of the spatial domain as indicated by the vertical dashed line.

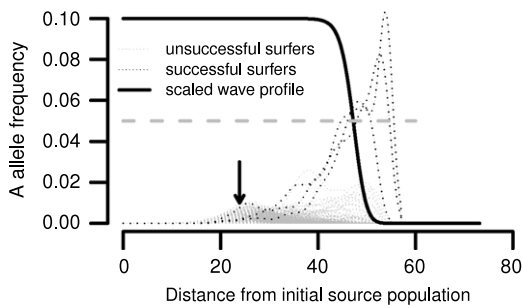


**Fig. 7.** In only three out of 1000 stochastic simulations with a Gaussian dispersal kernel, did the mutant allele achieve a frequency in the wave greater than 5% (horizontal dashed line) after it was introduced in the wave front. The figure shows stochastic realizations of the range expansion in Fig. 6(c) after 20 generations. Simulation parameters were  $R_0 = 10$ ,  $K = 40$ , and  $D = 0.8$ . In generation 11, a single A allele was introduced at the location indicated by the vertical arrow which represents the point in the traveling wave where the population density was approximately one individual per unit length of the spatial domain.

a wind field. Mountain pine beetles (*Dendroctonus ponderosae* Hopkins) in western Canada provide a good example of anisotropic expansion because they are undergoing a slow post-glacial range expansion to the North while rapidly invading eastward (Samarasekera et al., 2012). In our two-dimensional simulations, we found that heterozygosity retention was high in directions of faster range expansion relative to heterozygosity retention in directions of slower spread. Therefore, by sampling heterozygosity along transects, researchers may be able to infer the directions of fastest and slowest spread. Our findings suggest, however, that gradients in two-dimensional range expansions are much more subtle in the direction of spread, than in one dimensional range expansions. This is largely because a dispersal kernel with a given variance can lead to gene flow between many more demes in two-dimensional simulations than in one-dimensional simulations. Thus, our two-dimensional results reaffirm that deme

interconnectedness through dispersal is an important determinant of genetic diversity in expanding populations. In real populations, deme interconnectedness is likely impacted by factors such as landscape heterogeneity, the presence of movement corridors, and the size of the smallest habitable patch of land for a subpopulation.

Heterozygosity gradients may be obscured in empirical data due to sectoring. The sectoring phenomenon, in which sectors of a spatial domain are dominated by different genotypes in the absence of selection, has been observed in petri-dish experiments of spreading bacteria as well as in two-dimensional simulations (Hallatschek et al., 2007; Hallatschek and Nelson, 2010). Sectoring can lead to stronger changes in allelic distribution along transects perpendicular to axes of expansion than in the direction of expansion (Francois et al., 2010). Because we used Monte Carlo simulations to average over random changes in allelic frequency from one simulation to another, these sectoring patterns were not evident in our plots of simulation averages. However, they became evident when we plotted allelic distribution after a single stochastic run of our two-dimensional model. Therefore, to detect heterozygosity gradients along axes of range expansion in the presence of these stronger perpendicular gradients in allelic composition, researchers will need to average heterozygosity across many independently assorting loci, such as non-linked single nucleotide polymorphisms to remove stochastic sectoring patterns that will occur at any particular locus. Averaging over multiple independent loci in empirical data should yield similar results to averaging over multiple stochastic simulations as we have done.

Mutations in organisms that reproduce according to the laws of random mating were much less likely to reach frequencies higher than 5% than in simulations of range expansions in asexually reproducing organisms. Although our finding that 0.3% of introduced mutants establish at a frequency, higher than 5%, is high compared to what would be expected in a panmictic and static population of the same size, it is low compared to previously reported results.

**Table 1**

Standardizations used to compare range expansions with a variety of demographic growth parameters, dispersal parameters and redistribution kernels.

Standardization	Calculation	Figures
Speed	$2\sqrt{D \ln R_0}$	Figs. 1, 6
Variance	Given in text	Fig. 2
Spatial extent	Location of half maximum population size obtained numerically	Fig. 2(e)–(f)
Generations	–	Figs. 1, 2(a)–(c), 3, 4(d), 7, 8

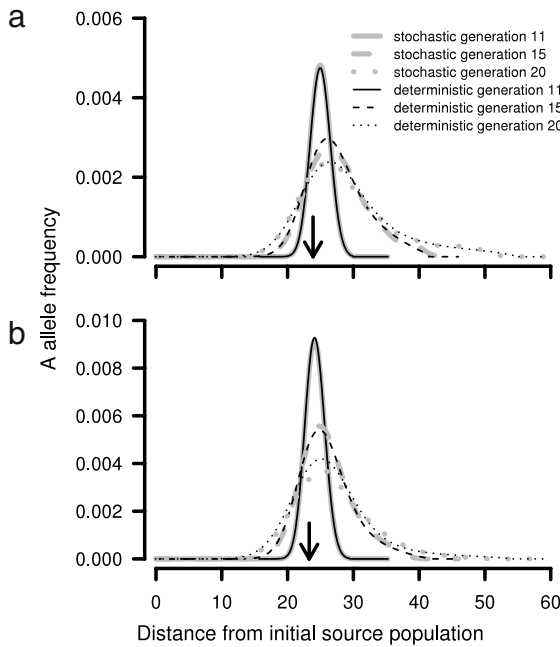


**Fig. 8.** The mean distribution of rare alleles that were initially introduced at the wave front is well predicted by deterministic models. Deterministic solutions (Eqs. (12) and (13)) are plotted over means of 100 stochastic simulations of range expansions in which all individuals initially possessed only the B allele. The dispersal kernel was a Gaussian kernel with  $D = 0.8$  and demographic growth parameters were  $R_0 = 10$ ,  $K = 40$ . Analogous range expansions were simulated with (a) random mating and (b) asexual reproduction. Simulations were initialized with 40 individuals at the origin and 40 individuals on either side of the origin all with a frequency of the A allele of 0. In generation 11, a single A allele was introduced at the location in the traveling wave where the population density was approximately one individual per unit length for the simulation with random mating and where the population density was approximately two individuals per unit length for the simulation featuring asexual reproduction. Thus, the initial frequency at which the A allele was introduced was  $\rho = 0.5$ .

Klopfstein et al. (2006) found that in 60% of new mutations occurring in the wave front of a simulation with similar maximum deme sizes ( $K = 50$ ), mutants increased to levels of 5%–50%. Stochastic birth processes in combination with kernels that widely distributed mutant alleles in our simulations resulted in low probabilities that a mutant allele would occur at levels high enough for it to flourish. To a lesser extent, this effect may have been observed in simulations reported by Klopfstein et al. (2006) who found that increased migration between demes decreased the prevalence of surfing mutant alleles. Our simulations imitate a highly connected and highly vagile species. In such systems, allele surfing seems to be less influential than in systems with narrow dispersal and asexual reproduction.

Distinguishing allele surfing from selection in empirical data remains difficult because allele surfing may generate false signals of selection. Our findings suggest that in genetic data arising from organisms that mate sexually and disperse widely, allele surfing should be much less prevalent than in asexually producing organisms with very localized dispersal. Therefore, in these types of organisms, researchers can be more confident in selection

results based on outlier detection even when both selection and surfing are possible. Positive selection, however, may enable rare alleles to surf where they otherwise would not, leading to interactive effects and further confusion. Surfing in combination with selection has been investigated in simulation studies (Travis et al., 2007; Hallatschek and Nelson, 2010).

It is important to distinguish between the rare occurrence of surfers that remain in the wave front and the overall distribution of mutant alleles after they occur at the front of range expansions. The latter can be represented using distributions that describe the mean behavior of mutant alleles in the population. In our simulations, distributions of mutant alleles at any time after they were introduced in the population wave were very well approximated using deterministic solutions of our integrodifference equation models. Therefore, any individual simulation in which alleles surfed to relatively high frequencies was balanced by a simulation where the same allele nearly drifted out of the population. When looking at a variety of independently assorting loci, for example in a single nucleotide polymorphism dataset in which linked loci have been removed, we expect that the mean frequency of any mutation will be well-represented by a deterministic model such as those described in our calculation section.

The distribution and diversity of neutral markers on the landscape can elucidate the history of populations as events and population characteristics become embedded in their collective DNA. Early on, researchers established the importance of population growth, and population mixing, in determining how much diversity is retained on landscapes (Wright, 1951; Nei et al., 1975; Malecot, 1975). These two components interact to determine the rate at which populations expand in space. As expansion tends to be anisotropic in real populations, direction-dependent information pertaining to invasion speed is therefore coded in their genetics—both in the loss of heterozygosity along the expansion axis, as well as in the prevalence of surfing and non-surfing mutations. Thus, interactions between growth and dispersal determine the genetic signature of range expansions such that in directions of fast invasion populations exhibit more gradual heterozygosity loss than in directions of slow expansion.

## Acknowledgments

We thank Ben Peter and two anonymous reviewers for helpful comments. Funding for this research was provided through grants to ML, DC, and BC from Genome Canada, from the Alberta government through Genome Alberta, and from the British Columbia government through Genome BC in support of The TRIA Project (<http://www.thetriaproject.ca>; grant number 1104), as well as from Alberta Innovates Bio Solutions through the Value Chain Sustainability Program (Grant number VCS-11-024).

## Appendix A. Standardizations

See Table 1.

## Appendix B. Supplementary data

Supplementary material related to this article can be found online at <http://dx.doi.org/10.1016/j.tpb.2014.08.005>.

## References

- Austerlitz, F., Dutech, C., Smouse, P.E., Davis, F., Sork, V.L., 2007. Estimating anisotropic pollen dispersal: a case study in *Quercus lobata*. *Heredity* 99 (2), 193–204.
- Austerlitz, F., JungMuller, B., Godelle, B., Gouyon, P., 1997. Evolution of coalescence times, genetic diversity and structure during colonization. *Theor. Popul. Biol.* 51 (2), 148–164.
- Beverton, R.J.H., 1957. *On The Dynamics of Exploited Fish Populations*. Chapman & Hall, London, UK.
- Bialozyt, R., Ziegenhagen, B., Petit, R., 2006. Contrasting effects of long distance seed dispersal on genetic diversity during range expansion. *J. Evol. Biol.* 19 (1), 12–20.
- Buerger, R., Akerman, A., 2011. The effects of linkage and gene flow on local adaptation: a two-locus continent-island model. *Theor. Popul. Biol.* 80 (4), 272–288.
- Codling, E.A., Plank, M.J., Benhamou, S., 2008. Random walk models in biology. *J. R. Soc. Interface* 5 (25), 813–834.
- DeGiorgio, M., Degnan, J.H., Rosenberg, N.A., 2011. Coalescence-time distributions in a serial founder model of human evolutionary history. *Genetics* 189 (2), 579–593.
- DeGiorgio, M., Jakobsson, M., Rosenberg, N.A., 2009. Explaining worldwide patterns of human genetic variation using a coalescent-based serial founder model of migration outward from Africa. *Proc. Natl. Acad. Sci. USA* 106 (38), 16057–16062.
- Edmonds, C., Lillie, A., Cavalli-Sforza, L., 2004. Mutations arising in the wave front of an expanding population. *Proc. Natl. Acad. Sci. USA* 101 (4), 975–979.
- Excoffier, L., Ray, N., 2008. Surfing during population expansions promotes genetic revolutions and structuration. *Trends Ecol. Evol.* 23 (7), 347–351.
- Francois, O., Currat, M., Ray, N., Han, E., Excoffier, L., Novembre, J., 2010. Principal component analysis under population genetic models of range expansion and admixture. *Mol. Biol. Evol.* 27 (6), 1257–1268.
- Gammon, D., Maurer, B., 2002. Evidence for non-uniform dispersal in the biological invasions of two naturalized North American bird species. *Global Ecol. Biogeography* 11 (2), 155–161.
- Gillespie, J.H., 2004. *Population Genetics – A Concise Guide*. Johns Hopkins, Baltimore, Maryland.
- Hallatschek, O., Hersen, P., Ramanathan, S., Nelson, D.R., 2007. Genetic drift at expanding frontiers promotes gene segregation. *Proc. Natl. Acad. Sci. USA* 104 (50), 19926–19930.
- Hallatschek, O., Nelson, D.R., 2008. Gene surfing in expanding populations. *Theor. Popul. Biol.* 73 (1), 158–170.
- Hallatschek, O., Nelson, D.R., 2010. Life at the front of an expanding population. *Evolution* 64 (1), 193–206.
- Hewitt, G., 1999. Post-glacial re-colonization of European biota. *Biol. J. Linnean Soc.* 68 (1–2), 87–112.
- Ibrahim, K., Nichols, R., Hewitt, G., 1996. Spatial patterns of genetic variation generated by different forms of dispersal during range expansion. *Heredity* 77 (3), 282–291.
- Kimura, M., Weiss, G., 1964. Stepping stone model of population structure and decrease of genetic correlation with distance. *Genetics* 49 (4), 561–576.
- Klopfstein, S., Currat, M., Excoffier, L., 2006. The fate of mutations surfing on the wave of a range expansion. *Mol. Biol. Evol.* 23 (3), 482–490.
- Kot, M., Lewis, M., vandenDriessche, P., 1996. Dispersal data and the spread of invading organisms. *Ecology* 77 (7), 2027–2042.
- Le Corre, V., Kremer, A., 1998. Cumulative effects of founding events during colonisation on genetic diversity and differentiation in an island and stepping-stone model. *J. Evol. Biol.* 11 (4), 495–512.
- Le Corre, V., Machon, N., Petit, R., Kremer, A., 1997. Colonization with long-distance seed dispersal and genetic structure of maternally inherited genes in forest trees: a simulation study. *Genet. Res.* 69 (2), 117–125.
- Lehe, R., Hallatschek, O., Peliti, L., 2012. The rate of beneficial mutations surfing on the wave of a range expansion. *PLoS Comput. Biol.* 8 (3), <http://dx.doi.org/10.1371/journal.pcbi.1002447>.
- Levin, S., Muller-Landau, H., Nathan, R., Chave, J., 2003. The ecology and evolution of seed dispersal: A theoretical perspective. *Annu. Rev. Ecol. Evol. Syst.* 34, 575–604.
- Malecot, G., 1975. Heterozygosity and relationship in regularly subdivided populations. *Theor. Popul. Biol.* 8 (2), 212–241.
- Morin, R.S., Liebhold, A.M., Gottschalk, K.W., 2009. Anisotropic spread of hemlock woolly adelgid in the eastern United States. *Biol. Invasions* 11 (10), 2341–2350.
- Munoz, J., Felicísimo, A., Cabezas, F., Burgaz, A., Martínez, I., 2004. Wind as a long-distance dispersal vehicle in the Southern Hemisphere. *Science* 304 (5674), 1144–1147.
- Nei, M., Maruyama, T., Chakraborty, R., 1975. Bottleneck effect and genetic variability in populations. *Evolution* 29 (1), 1–10.
- Neubert, M., Kot, M., Lewis, M., 1995. Dispersal and pattern formation in a discrete-time predator–prey model. *Theor. Popul. Biol.* 48 (1), 7–43.
- Nichols, R., Hewitt, G., 1994. The genetic consequences of long-distance dispersal during colonization. *Heredity* 72 (3), 312–317.
- Phillips, B.L., Brown, G.P., Travis, J.M.J., Shine, R., 2008. Reid's paradox revisited: the evolution of dispersal kernels during range expansion. *Amer. Nat.* 172 (1), S34–S48.
- R Core Team 2013. *R: A Language and Environment for Statistical Computing*. R Foundation for Statistical Computing, Vienna, Austria, ISBN: 3-900051-07-0, URL: <http://www.R-project.org/>.
- Ramachandran, S., Deshpande, O., Roseman, C., Rosenberg, N., Feldman, M., Cavalli-Sforza, L., 2005. Support from the relationship of genetic and geographic distance in human populations for a serial founder effect originating in Africa. *Proc. Natl. Acad. Sci. USA* 102 (44), 15942–15947.
- Roques, L., Garnier, J., Hamel, F., Klein, E.K., 2012. Allee effect promotes diversity in traveling waves of colonization. *Proc. Natl. Acad. Sci. USA* 109 (23), 8828–8833.
- Samarasekera, G.D.N.G., Bartell, N.V., Lindgren, B.S., Cooke, J.E.K., Davis, C.S., James, P.M.A., Coltman, D.W., Mock, K.E., Murray, B.W., 2012. Spatial genetic structure of the mountain pine beetle (*Dendroctonus ponderosae*) outbreak in western Canada: historical patterns and contemporary dispersal. *Mol. Ecol.* 21 (12), 2931–2948.
- Singleton, R., 1969. An algorithm for computing mixed radix fast Fourier transform. *IEEE Trans. Audio Electroacoust.* AU17 (2), 93–103.
- Skarpaas, O., Shea, K., 2007. Dispersal patterns, dispersal mechanisms, and invasion wave speeds for invasive thistles. *Amer. Nat.* 170 (3), 421–430.
- Slatkin, M., Excoffier, L., 2012. Serial founder effects during range expansion: a spatial analog of genetic drift. *Genetics* 191 (1), 171–181.
- Taylor, R., 1978. Relationship between density and distance of dispersing insects. *Ecol. Entomol.* 3 (1), 63–70.
- Thibault, I., Bernatchez, L., Dodson, J.J., 2009. The contribution of newly established populations to the dynamics of range expansion in a one-dimensional fluvial-estuarine system: rainbow trout (*Oncorhynchus mykiss*) in Eastern Quebec. *Diversity and Distributions* 15 (6), 1060–1072.
- Travis, J.M.J., Muenkemueller, T., Burton, O.J., Best, A., Dytham, C., Johst, K., 2007. Deleterious mutations can surf to high densities on the wave front of an expanding population. *Mol. Biol. Evol.* 24 (10), 2334–2343.
- Wallace, B., 1966. On dispersal of *Drosophila*. *Amer. Nat.* 100 (916), 551–563.
- Walters, R.J., Hassall, M., Telfer, M.G., Hewitt, G.M., Palutikof, J.P., 2006. Modelling dispersal of a temperate insect in a changing climate. *Proc. R. Soc. Lond. Biol.* 273 (1597), 2017–2023.
- Wright, S., 1951. The genetical structure of populations. *Ann. Eugenics* 15 (4), 323–354.